

RESEARCH ARTICLE

Finite element analysis of a stemmed hip prosthesis to reduce stress shielding in the proximal femur

Oliver Bliss¹, J. Greg Swadener^{1,*}, Gillian Pearce¹, and Iham F. Zidane²

¹ School of Engineering and Applied Science, Aston University, Aston Triangle, Birmingham, B4 7ET, U.K.

² Mechanical Engineering Department, College of Engineering and Technology, Arab Academy of Science, Technology and Maritime Transport (AASTMT), 1029 Abu Kir, Alexandria – Egypt

ABSTRACT - A finite element analysis (FEA) was performed on four prosthesis designs with different internal structures within identical prosthetic stem geometry. A novel hexagonal structure akin to one of the strongest structures in nature is used internally in the stem. The hip implant designs were then analyzed for an applied force of 3227 N. This force was selected because a typical gait cycle generates forces up to 3.87 times the body weight in the hip joint. The FEA results were compared for various stem designs with rectangular cross-sections. The design objective for a hip stem is to have a low stiffness and stress shielding together with a very high fatigue life. The stress shielding reduction of the prosthesis was measured by observing the change in stress distribution in a FE femur model before and after implant. Stress shielding was quantified volumetrically, and the surface stresses of the femur were considered to appraise any increased risk of periprosthetic fracture due to increased bone stress. Subsequently, the stems that had the lowest stress shielding models were then optimized. Results showed a reduction of stiffness of 18%, and a reduction in stress shielding of 30% compared to a solid stem.

ARTICLE HISTORY

Received : 25th Apr. 2022

Revised : 14th Nov. 2022

Accepted : 05th Jan. 2023

Published : 23rd Mar. 2023

KEYWORDS

Total hip replacement

Finite element analysis

Biomedical

Prosthesis stem

Proximal femur

1.0 INTRODUCTION

Numerous stem designs for total hip arthroplasty (THA) implants have been introduced over the last decades [1, 2]. It is questionable if small differences between the implant designs affect stress shielding and bone remodeling. The finite element analysis (FEA) allows an evaluation of the design justification of the implant without negative side effects for the patient. It is a well-established, reliable and efficient computing method. This technology can provide correlation of bone remodeling with stress patterns to examine phenomena derived from different implants [3, 4]. FEM can only work when it accurately predicts the process it was designed to replicate [2].

Stress shielding is caused by a difference in stiffness between a prosthesis and the stiffness of femoral bone, as bending stresses are not distributed through the femur in the same way as they were before implant. There have been many attempts to produce prosthesis designs to reduce stress shielding. Beulah et al. [5] was one of the early studies to use FEA to optimize the stem cross-sections. Arabnejad et al. [6] experimented by creating a porous prosthesis stem with varying material porosity to reduce stiffness of a prosthesis. The result of this study indicated a total reduction of 77% in bone reabsorption due to stress shielding via an FE femur model with a physical verification from an anatomical femur model. Caoutte et al. [7] use a carbon fibre composite stem to reduce stiffness and stress shielding. Fraldi, et al. [8] used a topological optimization method and was able to almost completely negate stress shielding at the diaphysis of the femur, although stress shielding in the trochanter was 15%. Singh and Tandon [9] produced a prosthesis with porosity (for fixation) made from 3 different titanium alloys, Ti64, TMZF and TMZTO which claimed to reduce stress shielding by 31%. He et al. [10] produced a lattice structure which was tested using the ISO 7206-4 standard loading conditions as well as having an FE model of an implanted femur, it was observed in the modelling that this prosthesis could reduce stress shielding to 10-16% compared to the natural femur, which was a 57.3% reduction compared to a solid stem. While these reductions in stress shielding are significant, the reduction in stress shielding cannot be compared directly between studies, because they start with different baselines. Instead, the maximum stress shielding relative to the natural femur can be used to compare between studies. The lowest stress shielding result achieved was the 15% stress shielding (induced in the trochanter) by Fraldi et al. Jetté, et al. [11] used an alternative approach creating a lattice structure which had pores of the right size to provide effective bone ingrowth for fixation as well as stiffness reduction, combining the benefits of lattice and porous structures. This design was observed to have around 30% lower stiffness than a solid prosthesis. Finally, Moussa, et al. [12] proposed a design using a reduced cross section to reduce stress shielding and cement damage at the cement-implant interface, by using computational optimization and then a further reduction using a construction from multiple lower stiffness materials. That study was successful in reducing stress shielding (although values are not reported), but their concept can only be used for cemented prostheses because of the reduced size of the stem generated.

In this study, the greatest load case is modelled following ISO 7206-4, which is the largest compressive load used (and following He et al. [10]). This load case is modelled, because it shows the greatest stress shielding, which is the critical problem the design is attempting to address. Other loading cases have lower stresses and show much less stress shielding, so the scope is limited to this one case to maintain the focus of this study. This paper investigates whether stress shielding and interface stresses can be controlled more effectively by the use of a hip prosthesis stem. Stems with different geometries are compared and the most promising ones used to generate improved designs using finite element analysis.

2.0 METHODS AND MATERIAL

A finite element analysis was undertaken on a simplified three-dimensional model of an uncemented hip prosthesis. The three-dimensional model was constructed and analyzed using ANSYS (ANSYS, Inc., Canonsburg, PA USA), a FEA package. All materials were assumed to be linear, elastic, and isotropic and all meshes were generated using quadratic tetrahedral elements. The FEA study is limited to the initial mechanical aspects and does not include biological effects such as bone growth and remodeling over time. Stress shielding is used as to provide an indication of the direction bone remodeling will take for the different stem designs.

2.1 Hip Prosthesis Design

The cross section of the prosthesis was chosen to be rectangular with 5mm radius fillets to reduce any stress concentrations caused by sharp corners when loaded. According to Noble, et al. [13], the typical dimensions for the cortical channel in the proximal femur is 2-5 mm to reduce micromotion. High levels of micromotion can lead to the development of fibrous tissue as opposed to bone ingrowth, which could negate the effects of an optimized prosthesis [14]. The anatomy is represented as using a classic resection at Total Hip Replacement (THR), that is the resection is made through the intertrochanteric line from the superior aspect of the greater trochanter to the lesser trochanter. The hip prosthesis neck angle in this study is as used in [15]. It is noted that during THR surgery, the bulk of the cancellous bone is removed during the operation. Consequently, the stem is placed into direct contact with cortical bone so that the load is directly transferred from the stem to the structural cortical bone. If cancellous bone were to carry any significant load, it would probably fail and result in the need for revision surgery. Therefore, the surgical procedure avoids placing cancellous bone under load. Consequently, our modelling does not need to consider cancellous bone. It is also noteworthy that previous papers in the literature have shown that the effects of cancellous bone are insignificant under static loading, e.g., Bougherara et al. [16]. Muscle and other soft tissue loads are also insignificant under compressive loading. The femoral head used in the modelling was chosen to be a 36mm diameter ceramic head. According to, Tsikandylakis et al. [17], 36mm Ceramic on Polymer (CoP) heads could help decrease risk of dislocation and improve stability.

Material selection for a prosthesis is key as the material used needs to be biocompatible. According to Choroszyński et al [18], the three main materials used for commercial hip replacements are Cobalt Chromium, Stainless Steel alloys and Ti64. Ti64 was chosen, in this prosthesis, as it has the lowest stiffness as shown in Table 1. According to this material selection, stress shielding would be minimized. Epoxy resin was used for the block to mount the prosthesis in [19].

Table 1. Biomaterials approximate mechanical properties [18]

Material	Young's Modulus (GPa)	Yield Strength (MPa)	Ultimate Tensile Strength (MPa)
Ti-6Al-4V	115	>730	>890
Cobalt alloys	230	>500	>600
Stainless steels	210	180-600	480-900

2.2 Internal Structure

For this prosthesis, a honeycomb structure of hexagonal channels was used to reduce prosthesis stiffness [20]. Four designs, as shown in Figure 1, were created using hexagonal channels of diameters between 1 – 4 mm with the total volume of the parts in all cases being 40,000 mm³ ±5% and the hexagonal shape allowing for a constant 1mm wall thickness around these channels. However, the femoral neck of the prosthesis was kept solid as this is one of the highest stress areas in the prosthesis and decreasing stiffness in that area could lead to yield or fatigue fracture.

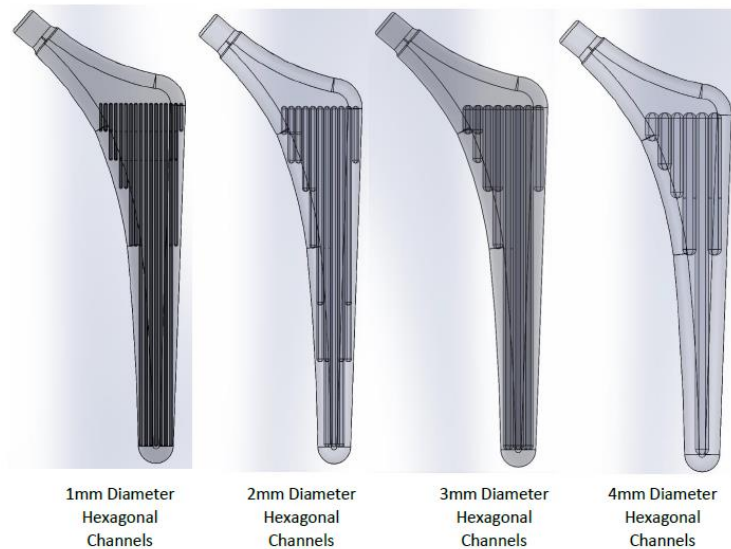


Figure 1. The internal structures created in this study

2.3 Static Loading Test

The loading conditions in the ISO 7206-4 test were selected as it provides a good indication of whether the prosthesis can stand up to loading conditions, although its primary use is to assess fatigue behavior of prosthesis designs [19]. The block used to mount the prosthesis in had a fixed restraint on the sides and bottom. A bonded contact was used between the prosthesis and the block. The mesh used was a 2mm mesh on the body of the prosthesis with refinements around the 0.5 mm fillets of the internal structure, the base of the neck, and the connection between the ball and the stem. The epoxy block, femoral head, and loading block had a 3mm mesh applied. The load selected was 3227 N which is 3.87 times the body weight for an 85 kg person. This body weight can occur when descending stairs and is one of the more extreme loading conditions [18]. Figure 2 shows the model mesh refinements.

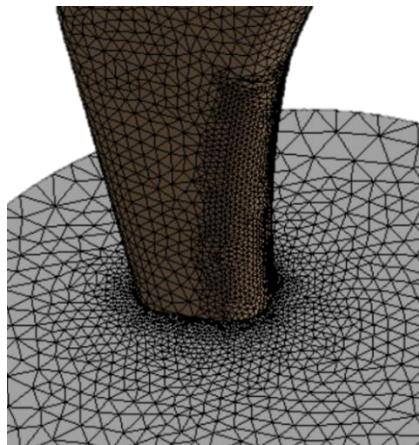


Figure 2. Model mesh refinements where the stem is inserted into the epoxy block

2.4 Femur Model

To assess stress shielding, a femur model, shown in Figure 3, was used enabling implants to be virtually inserted into and then loaded to predict how they would behave in use. Six analyses were performed, one using a femur without an implant, and one each for the 4 designs and the solid prosthesis. The model of the femur used was of a male cadaver specimen [21]. The model was simplified and the dimensions for the cortical channel were approximated as ellipses with sizes from data presented by Noble, et al. [13]. The same load as used in the static deflection test was applied vertically either as a surface load to the head of the femur or distributed on the femoral head of the prosthesis.

The model was split into 4 sections to facilitate evaluation of the average volumetric von Mises stress in specific sections of the femur (shown in Figure 4). The sections were modelled as separate bodies to ensure they would be identical in all tests and connected with bonded contacts. Higher average stresses in the femur would indicate less stress shielding and less susceptibility to bone loss. The interface is modelled as rigid contact between the stem and cortical bone, which is appropriate under compressive loading. No slip occurs in practice for >95% of cases. When slip does occur in practice, it is classified as a failure and usually requires revision. The mesh used was uniform and was made of either 1 mm or 1.25

mm elements (bar the 1mm diameter hexagonal structure) as the internal structures in the prosthesis required a considerable number of elements, preventing a 1mm element size being used throughout. All meshes were convergent within 2%, except for the 1 mm internal structure mesh, which was convergent within 4%. The Young’s modulus for cortical bone was set as 19.6 GPa [22].

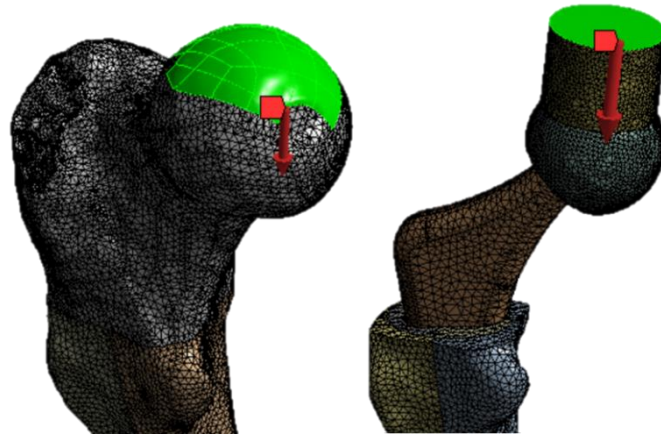


Figure 3. Application of loads applied to femur models in FEA

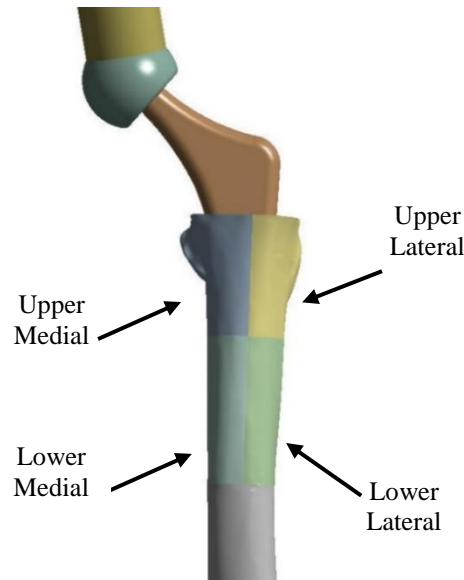


Figure 4. The split of the femur model into sections

3.0 RESULTS

3.1 FEA Loading and Deflection Results

The FE modelled ISO 7206-4 test was used to assess the maximum stress in the prosthesis when loaded, in addition to observing the deflection in the prosthesis under load. The maximum stresses in the prosthesis designs are shown in Table 2 together with the maximum deflections. The 2 mm and 3 mm structures had the highest maximum deflection; however, the 3 mm structure had a lower maximum stress induced with a greater safety factor to the maximum fatigue stress. The deflections in this table are maximum for the prosthesis stem and do not include the femoral head.

Table 2. Results from ISO static loading FE analysis

Design	Max Stress (MPa)	Max Deflection (mm)	Safety Factor to 410 MPa
Solid	318.22	1.0658	1.290
1mm	422.85	1.1695	0.970
2mm	399.16	1.3014	1.027
3mm	359.38	1.2734	1.140
4mm	325.39	1.1300	1.260

A key aspect of the design of a hip prosthesis is ensuring the prosthesis does not succumb to fatigue fractures. Hip prostheses undergo millions of loading cycles in use, the number of which increases when wanting to increase longevity of a prosthesis. If a patient takes 10,000 steps per day the prosthesis would undergo at least 5,000 cycles, and if the prosthesis needs to last over 30 years that would incur over 60 million loading cycles. The tests above show the prosthesis maximum stress is getting close to this level for some of the structures. However, the load used in the model was intended to be the maximum typical load expected, and the number of cycles at this load would be significantly lower than 60 million.

Solid prosthesis deflection, with the femoral head, was calculated to compare to Jetté et al. [11] and it was found to be 33.1% lower than tested in this study for vertical displacement. This is represented in Figure 5. The same boundary conditions were applied in both cases; however, the designs of the prostheses were different and will have deflected differently under load. The different geometries are the largest contribution to the observed differences observed in Figure 5. The method of the ISO test being used in FEA was observed by Jetté, et al. [11] to be within 6.1% of a physical verification, so if the discrepancy is just due to differences in design this would indicate that this analysis should be a good reflection of actual performance. However, without a physical verification it is hard to definitively state how well this analysis reflects the real condition. Figure 6 shows a graph of load vs deflection for the prostheses. The gradient of this line was then used to calculate the stiffnesses seen in Table 3, with the lowest stiffness being the 2 mm structure implant.

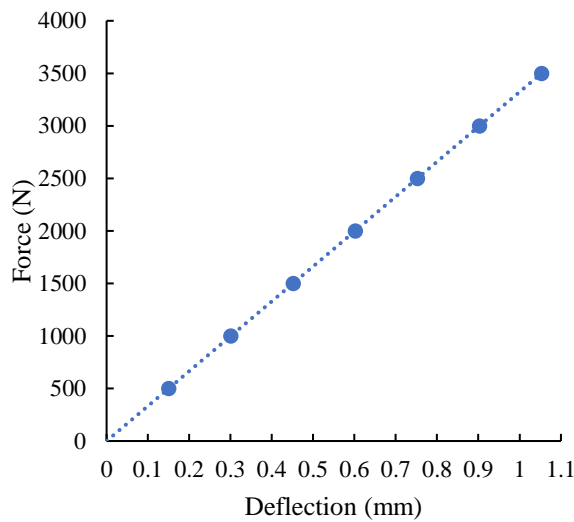


Figure 5. Load vs deflection for the solid prosthesis design with femoral head

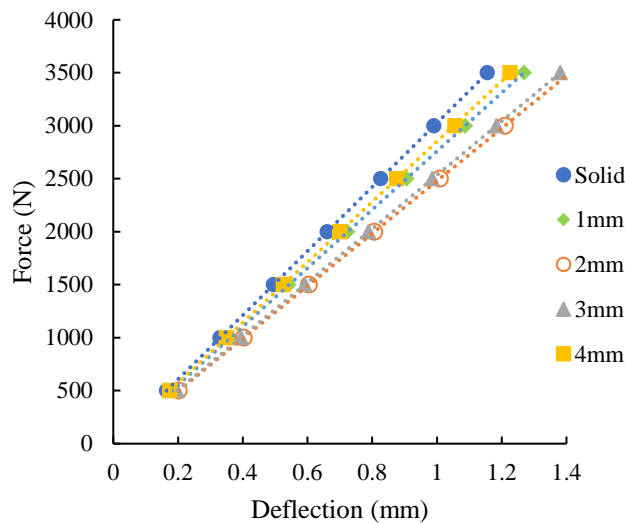


Figure 6. Force vs total deflection of prosthesis designs

Table 3. Calculated stiffness and stiffness reductions

Prosthesis	Stiffness (N/mm)	Percentage Decrease
Solid	3026.37	N/A
1mm	2759.71	8.8%
2mm	2480.07	18.1%
3mm	2534.39	16.3%
4mm	2848.80	5.9%

3.2 Stress Shielding Analysis

The average volumetric stress with a solid prosthesis implanted was compared to the femur without a prosthesis implanted to assess the degree of stress shielding induced. The percentage difference between the average values was taken to be the value of stress shielding induced, as shown in Table 4. Table 5 then shows the stress shielding induced in the segments by each prosthesis.

From the FE analysis carried out as shown in Table 5, it can be observed that the best prosthesis for decreasing stress shielding was the 3mm diameter internal structure. A reduction in average shear stress index (SSI [8]) from 21.5% to 14.7% for the stem gives a positive indication of this prosthesis' ability to reduce the effects of bone loss leading to aseptic loosening. According to Table 5, it can be seen that the 1mm diameter structure performed well at reducing stress shielding, despite having a poor stiffness reduction. However, the mesh used for the analysis with this structure was about 3 times less fine than the other meshes likely making it less accurate. The 1mm diameter hexagonal structure required lots of elements to be able to generate the mesh resulting in 683,658 elements in total, which is 300,000 more elements than used in the 4 mm internal structure model. Mesh convergence was within 2%.

Table 4. Average von Mises stress in femur regions for femur without implant and femur with solid prosthesis and 3227 N applied load

Section	Natural Femur Average Volumetric Stress (MPa)	Solid Prosthesis in Femur Average Stress (MPa)	Stress Shielding Induced (%)
Upper Medial	10.5	7.27	31.0
Upper Lateral	17.0	10.2	40.1
Lower Medial	15.1	15.5	-2.4
Lower Lateral	21.0	17.3	17.5

Table 5. Stress shielding in femur regions induced by prosthesis designs

Area of Femur	Stress Shielding Induced by Prosthesis Designs (%)				
	Solid Prosthesis	1 mm Diameter	2 mm Diameter	3 mm Diameter	4 mm Diameter
Upper Medial	31.0	13.9	19.5	21.8	21.9
Upper Lateral	40.1	29.5	32.9	33.9	36.7
Lower Medial	-2.4	1.3	-7.5	-9.9	-3.1
Lower Lateral	17.5	18.8	15.1	13.0	18.3
Average SSI	21.5	15.9	14.9	14.7	18.5
SSI Decrease		5.6	6.6	6.8	3.0

3.3 Surface Stresses

Another method of assessing reduction in stress shielding is comparing the surface stresses in the femur before and after implantation. Figure 7 shows the contour plots of Von Mises stress distribution in the proximal femur with and without implants. It can be seen from the contour plots that all prosthesis designs increase bone stress and that the closest to the ideal stress distribution is the 3 mm structure as it induces higher stresses further up the femur. These contour plots line up well with the volumetric stress shielding values with all prostheses inducing stresses with the 3 mm structure performing best. The SSI based on maximum stress is 14.3% for the 3 mm structure compared to its average SSI of 14.7%. For the entire femur diaphysis, the SSI is 0-1 %, which is the same as Fraldi et al. [8].

In all cases, stresses were observed in the lower section of the femur which the femur without an implant does not have, but this is likely due to the prosthesis ending in that section of the femur. To evaluate any increased risk of periprosthetic fracture by this stress increase, maximum principal stress contour plots were obtained, in Figure 8, to see if any areas of high tensile stress could be observed. In all analyses there were high stresses around the base of the femur due to the fixed restraint in the boundary conditions and so was those concentrations were discounted.

All prostheses appear to increase the stress around the diaphysis of the femur. The increase does not appear to be significantly higher than the femur without an implant. The tensile yield stress for cortical bone was found to be around 110 MPa from hydrated cadaver samples by [23]. All models in this study are shown to be under 110 MPa by a factor of approximately 2.75, so the prosthesis should not directly increase the risk of a fracture.

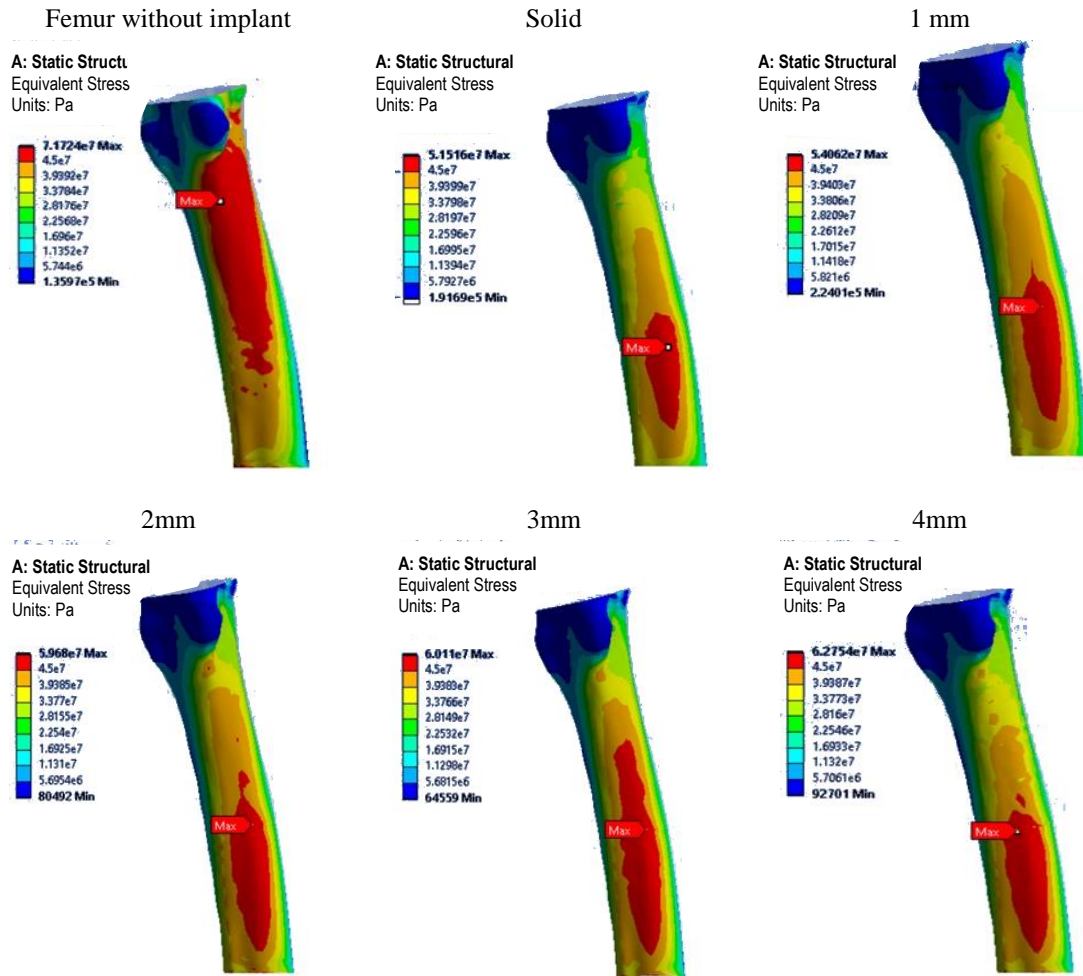


Figure 7. Stress contours and maximum Mises equivalent stress on the bone surface for the different hip stem designs

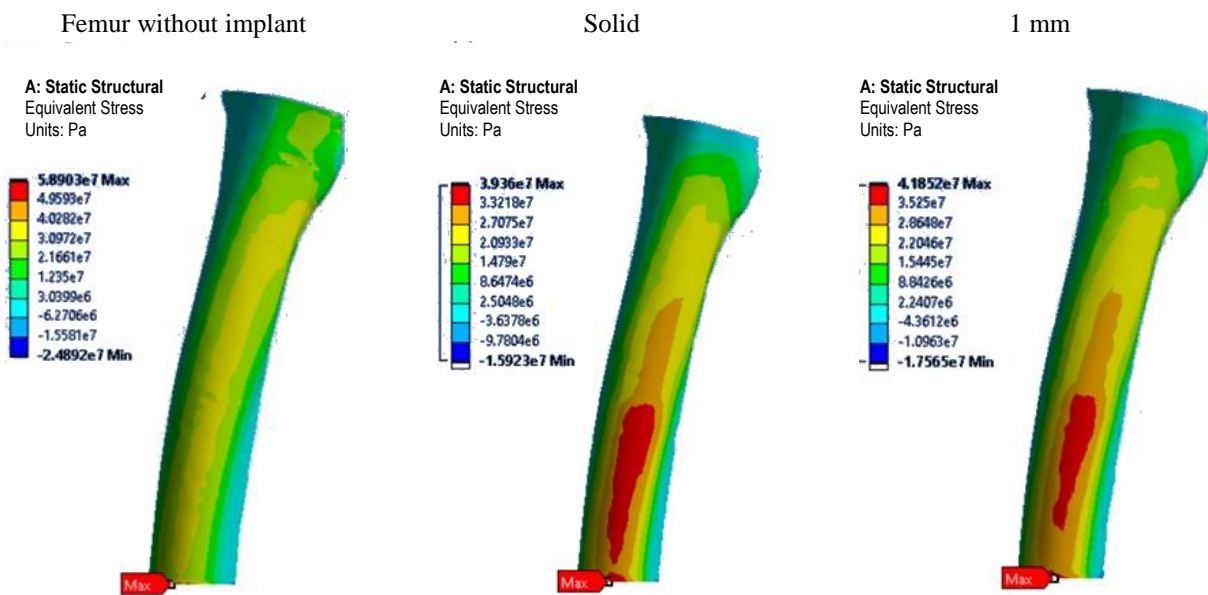


Figure 8. Tensile principal stress contours on the bone surface for the different hip stem designs

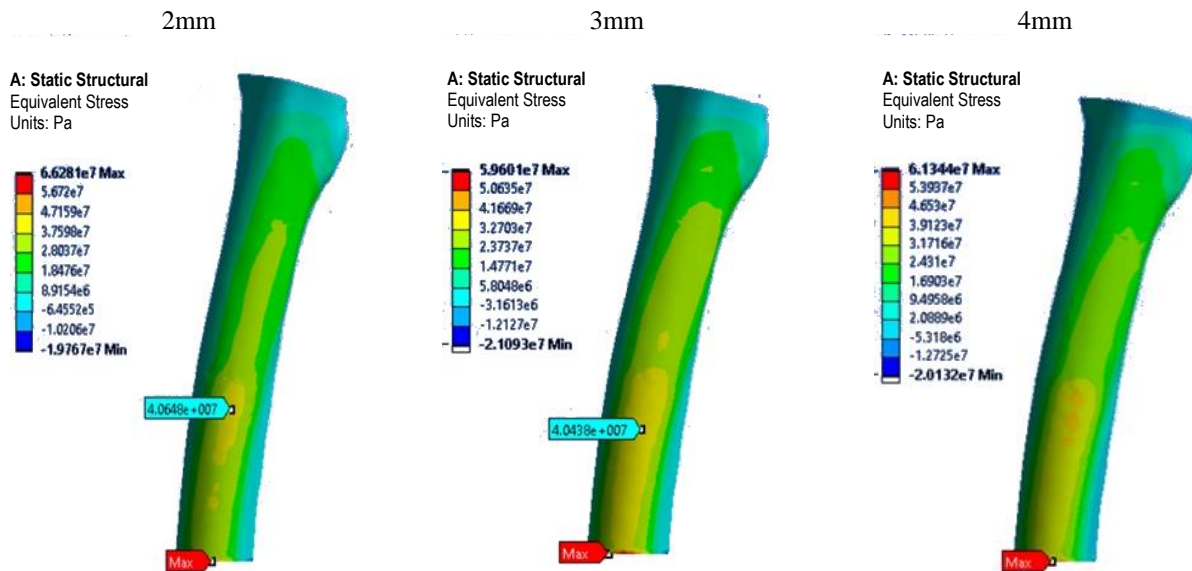


Figure 8. Tensile principal stress contours on the bone surface for the different hip stem designs (cont.)

4.0 DISCUSSION

Each FE analysis was checked for mesh convergence against the maximum stress and deformation and in all cases, the meshes were convergent within 2%. Figure 9 shows a graph of stress convergence for the solid prosthesis static loading test and shows good convergence but with some variation. This variation occurs because, as the mesh is refined, node positions change in the area of high stress, causing the interpolated maximum stress value to vary slightly. Figure 10 shows the deflection of the prosthesis and a much smoother convergence, which is why deflection was used as an additional step to verify mesh convergence. Figure 11 shows a graph of convergence of average stress in the different bone regions for the natural femur and solid prosthesis and shows good convergence. The average stress results for the other modules all lie in between the natural femur and the solid prosthesis. The static loading FE analysis showed that the maximum decrease in stiffness achieved was 18.1%. The FE analysis in the femur model showed that the prosthesis outlined in this study achieved an average stress shielding reduction of 30% in each of the sections sampled bar the lower lateral segment. From the structures analyzed in this study a 3 mm diameter appears to be the ideal size of the hexagonal channels, as it outperformed all the other prosthesis designs with a 6.8% reduction in stress shielding and with visual indications of a better stress profile seen from the Von Mises surface stress. The modelling of the stem structure is useful for evaluating the forces acting on the bone and gaining insight into how that honeycomb structure reacts under various conditions of loading. Also, the honeycomb structure we have modelled, could be used in stress testing, and we envisage in potentially growing bone cells themselves, using the honeycomb scaffold itself in order to grow new hip joints in the future. This will be the subject of our future research. Reduction in stress shielding, as mentioned previously, should lead to reduced bone loss better fixation and a reduced risk of aseptic loosening leading to greater prosthesis longevity. In turn, this would be expected to lead to lower cost for health services and fewer revision surgeries for patients due to aseptic loosening, although the exact impact would require a long-term study to quantify. In this study we note that we have modelled only the femoral component in order to compare hexagonal interiors of various sizes with a solid femoral stem, which is the current type of design in use in Total Hip Replacements. However future work will involve additional modelling and testing to compare the new construct with the classic totally solid structure of components currently used.

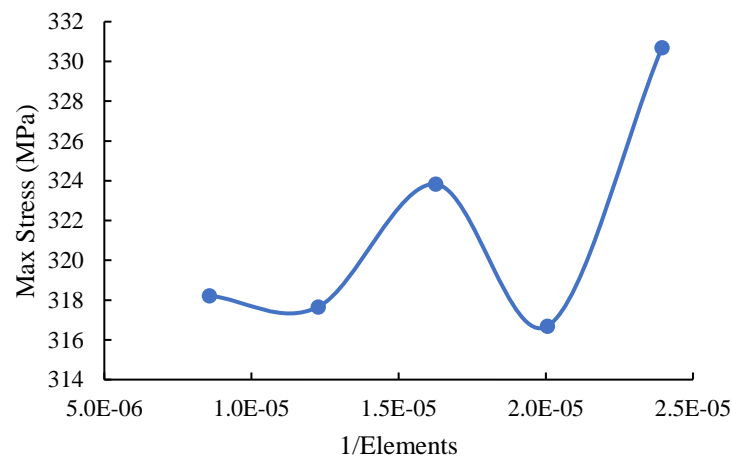


Figure 9. Mesh convergence of maximum Mises stress for the solid prosthesis and static loading

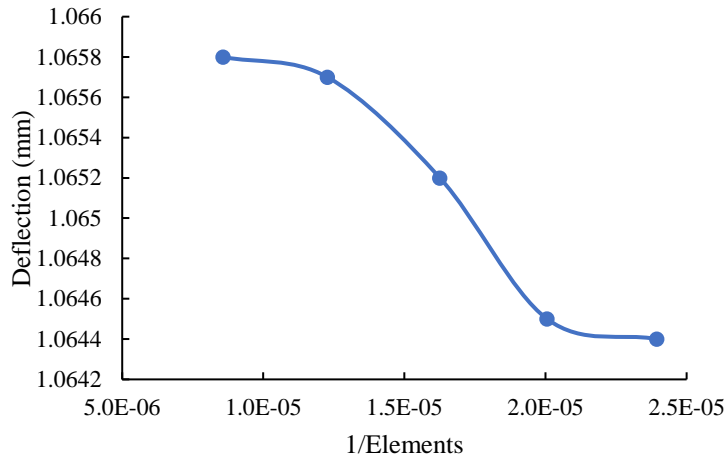


Figure 10. Mesh convergence of maximum deflection for the solid prosthesis

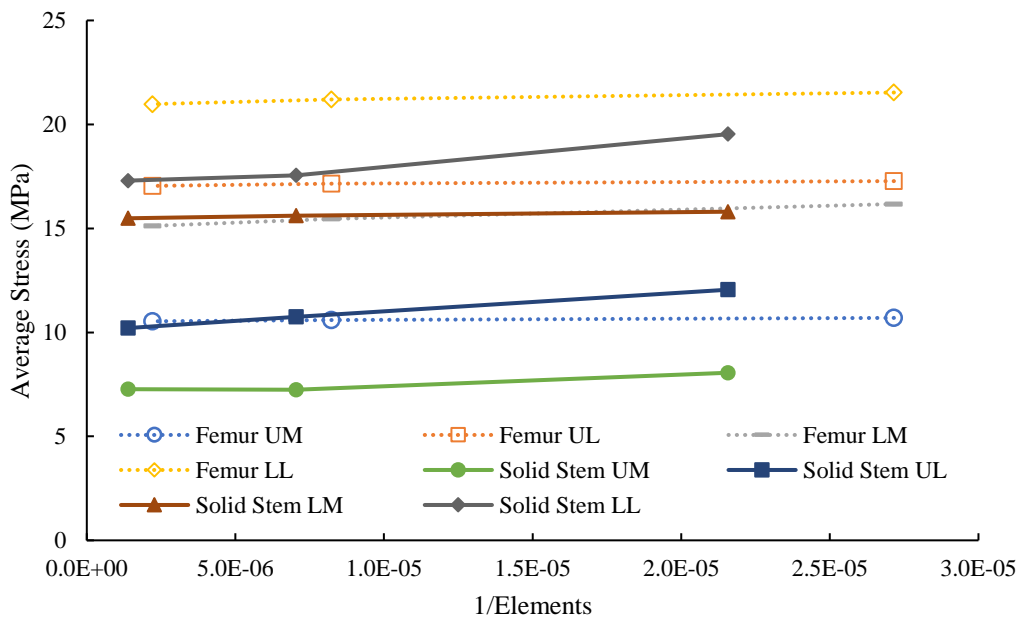


Figure 11. Mesh convergence of average stress for the upper medial (UM), upper lateral (UL), lower medial (LM), and lower lateral (LL) bone regions in the natural femur (dash lines) and solid stem (solid lines) prosthesis models

5.0 CONCLUSION

This study has outlined the design and finite element modelling of an uncemented prosthesis to reduce stress shielding in the proximal femur leading to aseptic loosening. It has been shown that by using hexagonal chambered internal structures stiffness can be reduced by around 18% and the effects of stress shielding can be reduced by 30.4% resulting in an average stress shielding index of 14.7%. This study has also highlighted that the ideal hexagonal structure with 3mm diameter hexagonal channels and 1 mm wall thickness can withstand the more severe loading conditions a prosthesis can expect without yielding and indicating it should also provide adequate fatigue strength.

This study was limited to a prototype design and more comprehensive testing and analysis is required before clinical studies can be started. However, the performance of the internal honeycomb structure performed better on stress shielding than the design in current use and shows sufficient promise to warrant more comprehensive studies. The potential patient benefits from reduced stress shielding are better integration with the bone and improved bone strength in the femur which would be expected lead to reduced aseptic loosening failures and improved patient recovery.

6.0 ACKNOWLEDGEMENT

This research received no external funding. Resources were provided by Aston University.

7.0 REFERENCES

- [1] S. B. Mirza, D.G. Dunlop, S. S. Panesar, S. G. Naqvi, S. Gangoo, and S. Salih, "Basic science considerations in primary total hip replacement arthroplasty," *The Open Orthopaedics Journal*, vol. 4, pp. 169-180, 2010.
- [2] M. Lerch, et al., "Finite element model of a novel short stemmed total hip arthroplasty implant developed from cross sectional CT scans," *Technology of Health Care*, vol. 21, pp. 493-500, 2013.
- [3] B. A. Behrens, I. Nolte, P. Wefstaedt, C. Stuckenberg-Colsman, and A. Bougeucha, "Numerical investigations on the strain-adaptive bone remodelling in the periprosthetic femur: Influence of the boundary conditions," *Biomedical Engineering Online*, vol. 8, p. 7, 2009.
- [4] J. Kerner et al., "Correlation between pre-operative periprosthetic bone density and post-operative bone loss in THA can be explained strain-adaptive remodelling," *Journal of Biomechanics*, vol. 32, pp. 695-703, 1999.
- [5] P. Beulah, S. Sivarasu, and L. Mathew, "Design optimization of skeletal hip implant cross-sections using finite element analysis," *Journal of Long-Term Effects of Medical Implants*, vol 19, pp. 271-278, 2009.
- [6] S. Arabnejad, B. Johnston, M. Tanzer, and D. Pasini, "Fully porous 3D printed titanium femoral stem to reduce stress-shielding following total hip arthroplasty," *Journal of Orthopaedic Research*, vol. 35, pp. 1774-1783, 2017.
- [7] C. Cauoette, L.H. Yahia, M. N. Bureau, "Reduced stress shielding with limited micromotions using a carbon fibre composite biomimetic hip stem: a finite element model," *Proceedings of the Institution of Mechanical Engineers, Part H: Journal of Engineering in Medicine*, vol. 225, no. 9, pp. 907-919, 2011.
- [8] M. Fraldi, L. Esposito, G. Perrella, A. Cutolo, and S. C. Cowin, "Topological optimization in hip prosthesis design," *Biomechincal Modelling and Mechanobiology*, vol. 9, no. 4, pp. 389-402, 2010.
- [9] S. K. Singh, P. Tandon, "Heterogeneous modeling-based prosthesis design with porosity and material variation," *Journal of the Mechanical Behavior of Biomedical Materials*, vol. 87, pp. 124-131, 2018.
- [10] Y. He, D. Burkhalter, D. Durocher, J. M. Gilbert, "Solid-lattice hip prosthesis design: Applying topology and lattice optimization to reduce stress shielding from hip implants," in *Proceedings of the 2018 Design of Medical Devices Conference*, DMD2018-6804, V001T03A001, 2018.
- [11] B. Jette, V. Brailovski, M. Durmas, C. Simoneau, P. Terriault, "Femoral stem incorporating a diamond cubic lattice structure: Design, manufacture and testing," *Journal of the Mechanical Behavior of Biomedical Materials*, vol. 77, pp. 58-72, 2017.
- [12] A. Ait Moussa, J. Fischer, R. Yadav, and M. Khandaker, "Minimizing stress shielding and cement damage in cemented Femoral component of a hip prosthesis through computational design optimization," *Advances in Orthopedics*, vol. 2017, p. 8437956, 2017.
- [13] P. C. Noble, J.W. Alexander, L. J. Lindahl, D. T. Yew, W. M. Granberry, and H. S. Tullos, "The anatomic basis of Femoral component design," *Clinical Orthopaedics, Related Research*, vol. 235, pp. 148-165, 1988.
- [14] K. A. Mann, M.A. Miller, P. A. Costa, A. Race, and T. H. Izant, "Interface micromotion of uncemented femoral components from postmortem retrieved total hip replacements," *Journal of Arthroplasty*, vol. 27, no. 2, pp. 65-75, 2012.
- [15] J. T. Kim, J. J. Yoo, "Implant design in cementless hip arthroplasty," *Hip & Pelvis*, vol. 28, no. 2, pp. 65-75, 2016.
- [16] H. Bougherara, M. Bureau, M. Campbell, A. Vadean, and L. H. Yahia, "Design of a biomimetic polymer-composite hip prosthesis," *Journal of Biomedical Materials Research A*, vol. 82A, pp. 27-40, 2007.
- [17] G. Tsikandylakis, M. Mohaddes, P. Cnudde, A. Eskelinen, J. Karrholm, and O. Rolfson, "Head size in primary total hip arthroplasty," *EFORT Open Review*, vol. 3, no. 5, p. 225-231, 2018.
- [18] M. Choroszyński, M.R. Choroszynski, and S. J. Skrzypek, "Biomaterials for hip implants – important considerations relating to the choice of materials," *Bio-Algorithms and Med-Systems*, vol. 13, no. 3, pp. 133-145, 2017.
- [19] British Standards Institute., "Determination of endurance properties and performance of stemmed femoral components," BS ISO 7206-4:2010+A1:2016. Part 4. BSI, 2016.
- [20] A. Ebrahinzadeh and N. Jamshidi, "Reducing stress shielding and weight as well as helping to revascularization of the Femur by applying honeycomb holes in hip prosthesis," *Journal of Mechanics in Medicine and Biology*, vol. 19, no. 06, p. 1950051, 2019.
- [21] M. Mahmoudi, M.R. Dorali, M. H. Beni, and H. Mahbadi, "Bio-CAD modelling of femoral bones with dual X-ray absorptiometry and spiral CT-scan technique," in *26th Annual International Conference of Iranian Society of Mechanical Engineers*. 2018. Semnan University, Semnan, Iran 24-26 April 2018.
- [22] J. Y. Rho, R.B. Ashman, and C.H. Turner, "Young's modulus of trabecular and cortical bone material: Ultrasonic and micro tensile measurements," *Journal of Biomechanics*, vol. 26, no. 2, pp. 111-119, 1993.

- [23] H. H. Bayraktar, E.F. Morgan, G. L. Niebur, G. E. Morris, E. K. Wong, and T. M. Keaveny, "Comparison of the elastic and yield properties of human femoral trabecular and cortical bone tissue," *Journal of Biomechanics*, vol. 37, no. 1, pp. 27-35, 2004.